frontiers | Frontiers in Chemistry

ORIGINAL RESEARCH
published: 30 June 2022
doi: 10.3389/fchem.2022.895483

Novel Coumarin–Pyridine Hybrids as Potent Multi-Target Directed Ligands Aiming at Symptoms of Alzheimer's Disease

Elaheh Babaei[1], Tuba Tüylü Küçükkılınç[2], Leili Jalili-Baleh[3], Hamid Nadri[4], Esin Öz[2], Hamid Forootanfar[5], Elaheh Hosseinzadeh[6], Tayebeh Akbari[7], Mehdi Shafiee Ardestani[8], Loghman Firoozpour[3], Alireza Foroumadi[3], Mohammad Sharifzadeh[9], Bi Bi Fatemeh Mirjalili[1] and Mehdi Khoobi[6,8]**

[1]Department of Chemistry, Faculty of Science, Yazd University, Yazd, Iran, [2]Department of Biochemistry, Faculty of Pharmacy, Hacettepe University, Ankara, Turkey, [3]Department of Medicinal Chemistry, Faculty of Pharmacy and Pharmaceutical Sciences, Tehran University of Medical Science, Tehran, Iran, [4]Faculty of Pharmacy, Shahid Sadoughi University of Medical Sciences, Yazd, Iran, [5]Department of Pharmaceutical Biotechnology, Faculty of Pharmacy, Kerman University of Medical Sciences, Kerman, Iran, [6]The Institute of Pharmaceutical Sciences (TIPS), Tehran University of Medical Sciences, Tehran, Iran, [7]Department of Microbiology, Islamic Azad University, North Tehran Branch, Tehran, Iran, [8]Department of Radiopharmacy, Faculty of Pharmacy, Tehran University of Medical Sciences, Tehran, Iran, [9]Department of Toxicology and Pharmacology, Faculty of Pharmacy, Tehran University of Medical Sciences, Tehran, Iran

OPEN ACCESS

Edited by:
Mina Saeedi,
Tehran University of Medical Sciences, Iran

Reviewed by:
Lhassane Ismaili,
Université Bourgogne Franche-Comté, France
Óscar López,
Sevilla University, Spain

***Correspondence:**
Bi Bi Fatemeh Mirjalili
fmirjalili@gmail.com
Mehdi Khoobi
m-khoobi@tums.ac.ir
mehdi.khoobi@gmail.com

Specialty section:
This article was submitted to Medicinal and Pharmaceutical Chemistry, a section of the journal Frontiers in Chemistry

Received: 13 March 2022
Accepted: 16 May 2022
Published: 30 June 2022

Citation:
Babaei E, Küçükkılınç TT, Jalili-Baleh L, Nadri H, Öz E, Forootanfar H, Hosseinzadeh E, Akbari T, Ardestani MS, Firoozpour L, Foroumadi A, Sharifzadeh M, Mirjalili BBF and Khoobi M (2022) Novel Coumarin–Pyridine Hybrids as Potent Multi-Target Directed Ligands Aiming at Symptoms of Alzheimer's Disease. Front. Chem. 10:895483. doi: 10.3389/fchem.2022.895483

In this research, a series of coumarin-based scaffolds linked to pyridine derivatives *via* a flexible aliphatic linkage were synthesized and assessed as multifunctional anti-AD agents. All the compounds showed acceptable acetylcholinesterase (AChE) inhibition activity in the nanomolar range (IC_{50} = 2–144 nM) and remarkable butyrylcholinesterase (BuChE) inhibition property (IC_{50} = 9–123 nM) compared to donepezil as the standard drug (IC_{50} = 14 and 275 nM, respectively). Compound **3f** as the best AChE inhibitor (IC_{50} = 2 nM) showed acceptable BuChE inhibition activity (IC_{50} = 24 nM), 100 times more active than the standard drug. Compound **3f** could also significantly protect PC12 and SH-SY5Y cells against H_2O_2-induced cell death and amyloid toxicity, respectively, superior to the standard drugs. It could interestingly reduce β-amyloid self and AChE-induced aggregation, more potent than the standard drug. All the results suggest that compound **3f** could be considered as a promising multi-target-directed ligand (MTDL) against AD.

Keywords: Alzheimer's disease, cholinesterase inhibitors, coumarin derivatives, neurodegenerative diseases, docking study

HIGHLIGHTS

- Twenty novel coumarin–pyridine hybrids were synthesized as anti-Alzheimer agents
- All the synthesized compounds were assessed for their anti-cholinesterase activity, and all of them indicated acceptable inhibitory activity
- Compound **3f** was the most influential compound against AChE
- Compound **3f** was more active than standard drugs in the protection of PC12 and SH-SY5Y cells against H_2O_2-induced cell death and amyloid toxicity, respectively

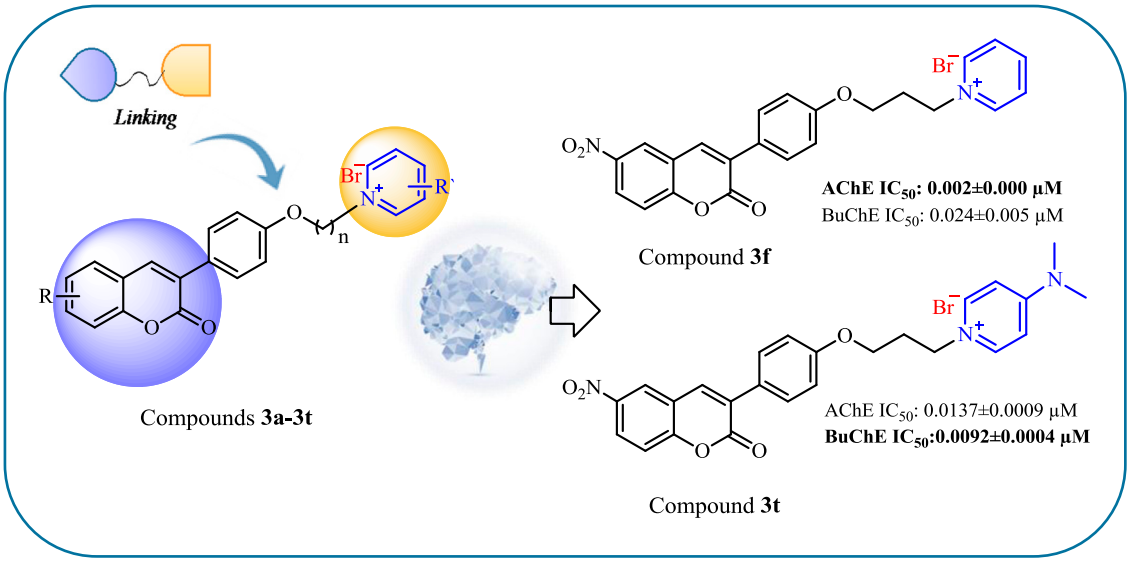

GRAPHICAL ABSTRACT | A novel series of 3-phenyl-coumarin derivatives containing pyridinium salts was prepared, indicating significant inhibitory activity against AChE and BuChE as well as precious neuroprotective and anti-Aβ aggregation effects.

- Compound **3f** was superior to the standard drug in the reduction of ß-amyloid self and AChE-induced aggregation

1 INTRODUCTION

Alzheimer's disease (AD) is a destructive neurodegenerative irregularity affecting memory, way of thinking, speaking, and other behavioral activities (Wang et al., 2014). Today, millions of people are afflicted with this disease, and the number is projected to increase in the next few years (Sang et al., 2018). Different factors such as inflammation, reduced acetylcholine (ACh) concentration, β-amyloid (Aβ) plaque formation, τ-protein aggregation, and oxidative stress cause AD, while the main reason is not perfectly understood (Patel et al., 2020). One of the most significant factors is the declined cholinergic activity resulting from ACh degradation by acetylcholinesterase (AChE), which affects memory loss. Conventionally approved drugs are mostly AChE inhibitors, increasing the amount of ACh in the synapses and decelerating the advancement of AD (Reddy et al., 2017; Li et al., 2018; Patel et al., 2020). Moreover, studies on the structure of AChE have indicated that it has two main sites for binding, including a peripheral anionic site (PAS) and a catalytic anionic site (CAS). AChE inhibitors binding to these two sites are more influential than the inhibitors occupying just one site of the enzyme. Butyrylcholinesterase (BuChE) has also had a great effect on the advancement of AD. BuChE inhibitors could retrieve cholinergic activity via restoring the proportions of AChE/BuChE activity like in a normal brain (Liu et al., 2020). As a consequence, dual AChE/BuChE inhibitors have drawn great interest in the management of AD (Davidsson et al., 2001).

On the other hand, AD is a continuing dementia equated by selective neuronal cell demise, which is undoubtedly triggered by Aβ fibrils or oligomers (Selkoe and Hardy, 2016; Murakami et al., 2020; Trambauer et al., 2020). Furthermore, several biomedical studies have shown that AChE promotes formation of amyloid fibril and creates extremely poisonous AChE-Aβ complex throughout the peripheral anionic site (PAS) (Inestrosa et al., 2005; Pradhan et al., 2018). Controlling Aβ protein formation or aggregation has a significant role in the enhancement of AD (Zou et al., 2015; Vyas et al., 2018). In primary steps of the degenerative nerve process, Aβ could go into the mitochondrion and escalate the creation of reactive oxygen species (ROS) by interrupting the electron transport chain, provoking oxidative stress (Chen et al., 2016; Yang et al., 2020). Hence, inhibition of Aβ accumulation, and therefore the formation of free radicals or preserving the cells against oxidative stress by neuroprotective agents, will be a propitious approach for the management of AD.

Advancement of multi-target-directed ligands (MTDLs) is one of the most encouraging drug discovery methods for ailments with a complex nature like AD. Mono-targeted medicines could not forever amend the complex ailing system sufficiently, even if these compounds regulate their targets with extreme selectivity and affinity (Zhang et al., 2016; Alcaro et al., 2019; González et al., 2019; Li et al., 2020). MTDLs have a superior capability to exert influence on the complicated balance of entire cellular network than single-targeted drug due to their synchronous consequences on various curative targets. Another positive aspect of these beneficial drugs is that they have a greater efficiency/security ration than a one-targeted drug (Bolognesi et al., 2011; Xuan et al., 2021). Consequently, there is a necessity to design suchlike compounds that can be effective on diverse relevant targets of AD, concurrently. These kinds of properties can be presumably attained by the linkage of diverse active moieties impacting on several targets. The linking hybrids with impression on distinctive targets might be advantageous to treat a complicated disorder like AD (Cavalli et al.,

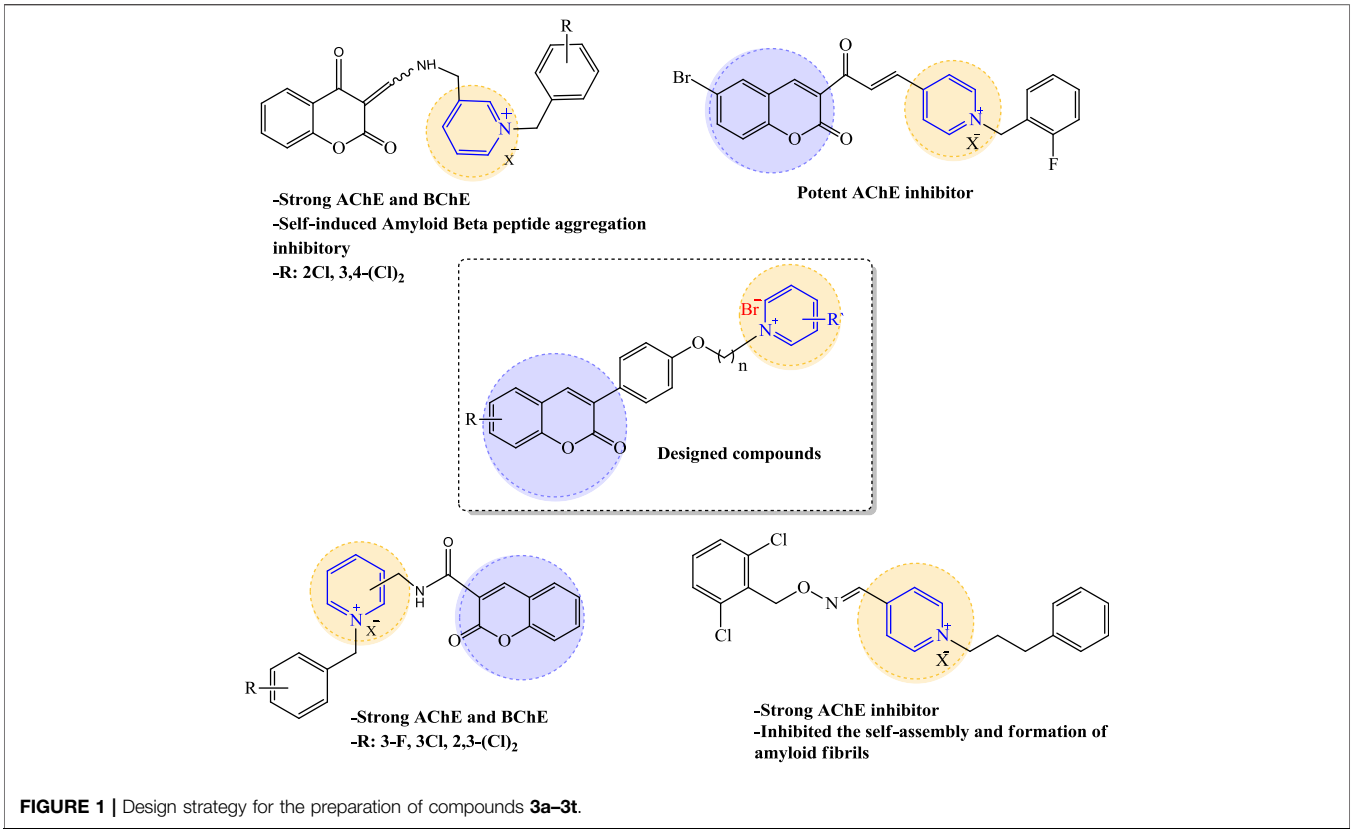

FIGURE 1 | Design strategy for the preparation of compounds **3a–3t**.

2008; Du et al., 2019; Sharma et al., 2019). Hitherto, the only three available ChE inhibitors prescribed for AD management (donepezil, rivastigmine, and galantamine) are single-target compounds inhibiting only ChEs. But they have no appropriate efficacy and may not be clinically significant (Marucci et al., 2021). In addition, so-called "drug-cocktails" like Memantine plus cholinesterase inhibitors are used in patients with advanced disease to pharmacologically treat these pathologies, with concerns related to drug-drug interactions as well as patient compliance (Chen et al., 2017). Hence, according to the paradigm of "network pharmacology," further research is needed to find novel bioactive compounds with multi-target properties (Hopkins, 2008; Chen et al., 2017). Irrevocably, treating AD and other neurodegenerative disease has been one of the major focal points of multi-target drug discovery procedures in the past 20 years.

A wide range of coumarin derivatives has been associated with an antioxidant trait (Bilgin et al., 2011; Anand et al., 2012; Pérez-Cruz et al., 2018; Koyiparambath et al., 2021). Some of which are identified to be active as AChE inhibitors and, as a consequence, could be noticed as a candidate with potential for the management of AD (Canning et al., 2013; Nasr et al., 2014; Bagheri et al., 2015). Additionally, a coumarin-based molecule, ensaculin, which contains benzopyran with the substitution of a piperazine, was introduced with the ability to enhance cognition and memory functions (Witaicenis et al., 2014; Abu-Aisheh et al., 2019).

On the other hand, investigations have been focused on the pyridine moiety because of its biological properties such as antioxidant and anti-inflammatory activities (Altaf et al., 2015). Furthermore, pyridinium salt has a well-known role in pharmacological interaction such as potent binding attraction in the direction of catalytic active site (CAS) of AChE by usage of charge interactions, π-stacking and therefore diverse MTDLs creating suchlike moiety have been reported so far (Kapková et al., 2006; Vafadarnejad et al., 2018; Mollazadeh et al., 2019).

In this work and in progression of our interest in the development of potent multi-target derivatives against AD (Choubdar et al., 2019; Abdpour et al., 2021), novel coumarin derivatives cross-linked with pyridinum salts were designed and synthesized by a simple procedure, resulting in a high yield. We focused on improving ChE inhibition of the coumarin-pyridinium backbone via a range of derivatives with donor/acceptor properties of the substituents, along with a flexible carbon chain as a linker to dedicate the structure of the target molecules with proper binding attraction and flexibility towards ChE enzymes as well as anti-Aβ aggregation and neuroprotective activities (**Figure 1**). We hope we can pave the way for rational and potent multi-target small molecule discovery in AD management, free from concerns about the cost, safety, and tolerability profile of the peptides and antibodies (Jeremic et al., 2021).

2 RESULTS AND DISCUSSION

2.1 Chemistry

All products were synthesized using commercially available 4-Hydroxyphenylacetic acid. Compound **1** was initially synthesized

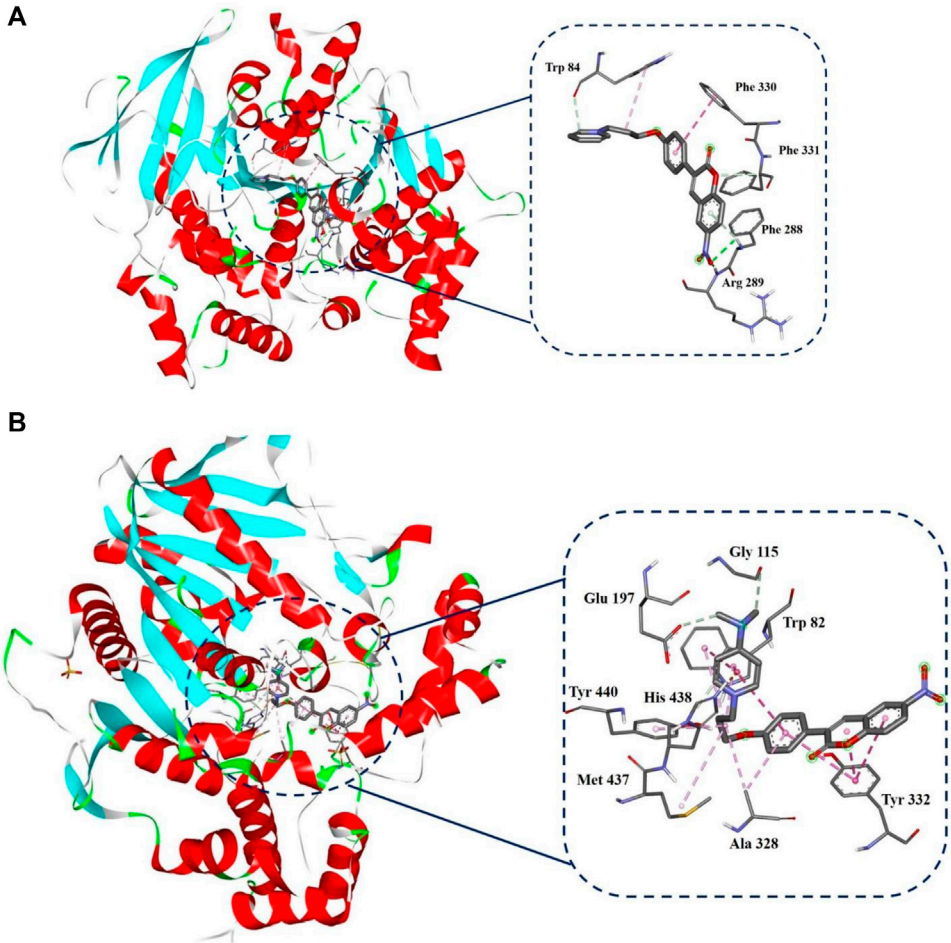

SCHEME 1 | Molecular docking of AChE **(A)** and BuChE **(B)** binding with compounds 3f and 3t, respectively.

via the reaction of 4-hydroxyphenylacetic acid with different salicylaldehyde derivatives in the presence of sodium acetate (NaOAc) in acetic anhydride (Ac_2O) under reflux conditions. The intermediate **1** was then reacted with an excess amount of various alkyl dibromides, potassium carbonate (K_2CO_3) in dry acetone under reflux condition, followed by reaction with different substituted pyridine in neat condition at 80°C to obtain the desired target compounds **3a**-**q** (**Scheme 1**). Also, products **3r-t** were directly synthesized from the reaction of compound **2** with 4-dimethylaminopyridine in dry acetonitrile under reflux conditions. All the reactions were monitored by TLC, and the products were purified simply by adding ether to the reaction solution. IR, ^{1}H and ^{13}C NMR spectroscopy were utilized for the product characterization.

2.2 Biological Assays

2.2.1 Anti-Cholinesterase Activity

To evaluate the anti-AD activity of the target compounds, their abilities to inhibit AChE and BChE were evaluated. All derivatives were screened for their *in vitro* AChE and BChE inhibitory properties (**Table 1**). The results showed that all the tested compounds were much more effective than Donepezil as the standard drug, with excellent AChE inhibitory activity in the nano-molar range. In particular, compounds **3p**, **3l**, **3a**, **3b**, **3c**, and **3g** showed inhibitory activities with IC_{50} values of 3, 3, 4, 4, 7, and 7 nM respectively. Compound **3f,** as the best AChE inhibitor with an IC_{50} value of 2 nM, was 7 times more active than the standard drug, Donepezil. The results revealed that 3-carbon chain length ($n = 3$) could be considered as the optimum length of the linker for AChE inhibition and that elongation of the linker led to a decrease in the activity. Also, the presence of different substituents at the phenyl ring of the coumarin moiety (R) had no effective role in improvement of the inhibitory effect, except for the nitro group on the 6-position of the coumarin ring in compounds **3f** and **3l,** which were the most potent compounds. However, increasing the length of the linker (n = 5, compound **3o**) and the presence of a 4-dimethylamine group at the para position of the pyridinium ring (compound **3t**), reduced the AChE inhibitory effect of the compounds having a 6-NO_2 group. We also investigated the BuChE inhibitory activity of the

TABLE 1 | Inhibitory activity of the target compounds **3a-t** against AChE and BuChE.

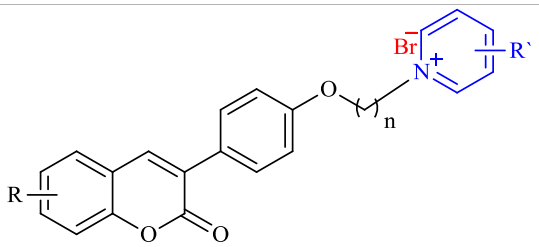

3a-t

Compound	nc	R	R′	AChE IC_{50} (nM)a	BuChE IC_{50} (nM)b
3a	3	H	H	4.0 ± 0.0	84.0 ± 4.0
3b	3	6-OMe	H	4.0 ± 1.0	68.0 ± 6.0
3c	3	7-OMe	H	7.0 ± 1.0	57.0 ± 10.0
3d	3	8-OMe	H	81.0 ± 4.0	79.0 ± 9.0
3e	3	6-Br	H	15.0 ± 3.0	33.0 ± 5.0
3f	3	6-NO_2	H	2.0 ± 0.0	24.0 ± 5.0
3g	4	H	H	7.0 ± 1.0	91.0 ± 18.0
3h	4	6-OMe	H	1003 ± 37.0	106.0 ± 8.0
3i	4	7-OMe	H	144.0 ± 9.0	46.0 ± 1.0
3j	4	8-OMe	H	31.0 ± 5.0	97.0 ± 19.0
3k	4	6-Br	H	40.0 ± 5.0	92.0 ± 9.0
3l	4	6-NO_2	H	3.0 ± 1.0	59.0 ± 11.0
3m	5	H	H	72.0 ± 8.0	86.0 ± 10.0
3n	5	8-OMe	H	15.0 ± 2.0	123.0 ± 24.0
3o	5	6-NO_2	H	22.0 ± 4.0	27.0 ± 2.0
3p	5	6-Br	H	3.0 ± 0.0	49.0 ± 5.0
3q	5	6-Br	5-Ethyl-2-Methyl	19.0 ± 1.6	22.0 ± 2.3
3r	5	6-Br	4-Dimethylamine	26.0 ± 2.1	52.0 ± 3.6
3s	3	H	4-Dimethylamine	22.0 ± 1.9	34.0 ± 2.6
3t	3	6-NO_2	4-Dimethylamine	14.0 ± 0.9	9.0 ± 0.4
Donepezil				14.0 ± 3.0	2,750 ± 205.0

[a]*Inhibitor concentration (mean ± SEM of three experiments) required for 50% inactivation of AChE (electric eel).*
[b]*Inhibitor concentration (mean ± SEM of three experiments) required for 50% inactivation of BuChE (equine serum).*
[c]*Length of linker (*n *= 3, 4, 5).*

isolated compounds (**Table 1**). Most of the compounds had high BuChE inhibition activity in the range of 22–123 nano-molar. But compound **3t** exhibited remarkable BuChE inhibitory activity with an IC_{50} = 9 nM, 305 times more active than the standard drug, Donepezil (BuChE IC_{50} = 2,750 nM). Compounds **3a-b, 3f-g, 3l, and 3t** as the best AChE and BuChE inhibitors were selected for further analysis.

2.2.2 Ligand–Protein Docking Simulation

To have a deep understanding of the interactions of potent compounds (**3f** and **3t**) with AChE and BuChE targets, respectively, docking simulation was carried out (**Figure 2**). In the case of AChE, compound **3f** showed interactions with Trp84 at the anionic site, hydrophobic Pi-Pi stacking interactions with Phe330 and two hydrogen bonds with Phe288 and Arg289 with the nitro group (**Figure 2A**). Therefore, compound **3f** inhibited AChE through hydrophobic interactions, and it was stabilized in the active site through hydrogen bonds.

Regarding the most active BuChE inhibitor, compound **3t** showed Pi-Pi stacking interactions with Tyr332 and Trp82 residues, Pi-cation interactions with His438 in the vicinity of the pyridinium region with positive charge, and Van der Waals interactions with Phe329, Pro285, Ser79, Gly78, Trp430, Gly439, Tyr128, Gly116, and Asp70 residues (**Figure 2B**). Therefore, it seems that hydrophobic interactions are responsible for the interactions of BuChE with compound **3t**.

2.2.3 Neuroprotection Assay Against H_2O_2-Induced Cell Death in PC12 Cells

The neuroprotective effects of compounds **3a-b, 3f-g, 3l, and 3t** at the concentrations of 0.1, 1, 5, 10, 20, and 50 μM against neurotoxicity caused by H_2O_2 were evaluated on neuroblastic PC12 cells. All the tested concentrations increased PC12 cell viability in a concentration-dependent manner (**Table 2**). Compounds **3a**, **3f**, **3l,** and **3t** showed a greater effect on cell viability, especially at low concentrations. Notably, the neuroprotective effects of compounds **3f** and **3l** at all concentrations were higher than those of the reference drug, Quercetin.

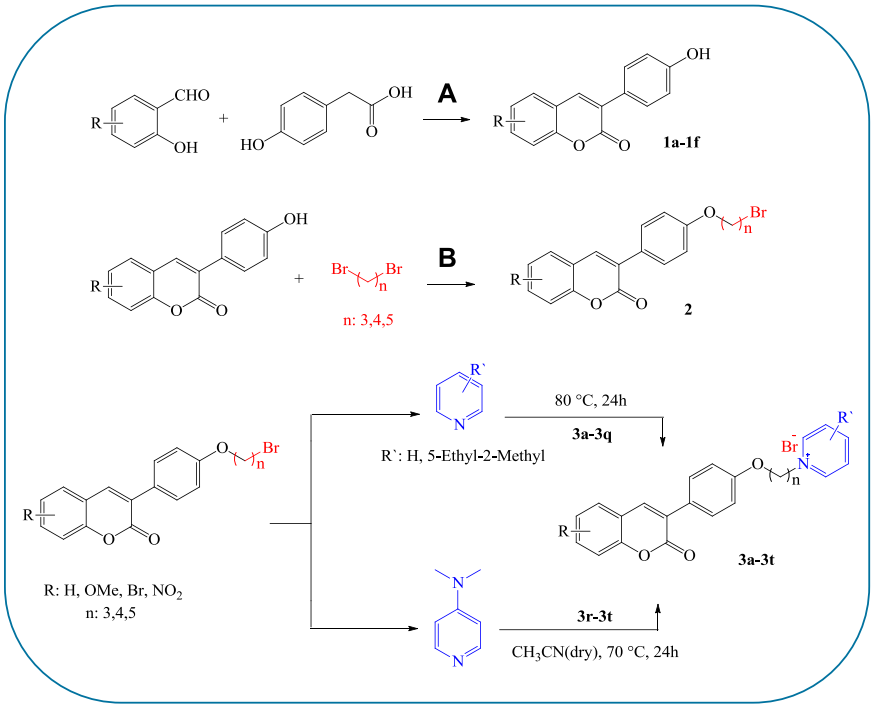

FIGURE 2 | Synthesis of target compounds 3a–t. **(A)** Ac_2O/NaOAc/Reflux 4–6 h, **(B)** K_2CO_3/acetone (dry)/Reflux 4 h

TABLE 2 | The protective effect of compounds 3a, 3b, 3f, 3g, 3l, and 3t against H_2O_2 (150 μM)-induced injury in the PC12 cell line at different concentrations in comparison to Quercetin[a].

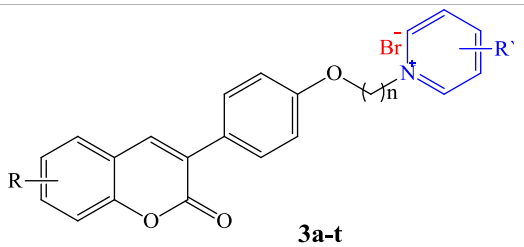

				PC12 cell viability (% of control)						
Compound	**n**	**R**	**R′**	**H_2O_2**	**0.1 μM**	**1 μM**	**5 μM**	**10 μM**	**20 μM**	**50 μM**
3a	3	H	H	26.7 ± 0.8	39.4 ± 1.7	42.2 ± 1.3	53.6 ± 1.4	55.6 ± 0.1	57.4 ± 0.4	58.3 ± 1.4
3b	3	6-OMe	H	26.2 ± 0.2	31.7 ± 1.4	37.6 ± 1.1	43.3 ± 0.9	45.4 ± 1.3	49.6 ± 0.9	54.3 ± 1.6
3f	3	6-NO_2	H	25.4 ± 1.5	34.1 ± 1.0	42.8 ± 1.4	43.1 ± 1.5	45.0 ± 0.8	48.3 ± 0.4	50.8 ± 0.6
3g	4	H	H	25.5 ± 0.7	30.2 ± 1.4	33.6 ± 1.2	36.6 ± 0.9	45.8 ± 0.3	48.7 ± 0.9	49.9 ± 0.9
3l	4	6-NO_2	H	23.5 ± 1.0	23.7 ± 0.5	27.3 ± 1.2	33.5 ± 1.2	37.8 ± 1.0	51.6 ± 1.1	55.7 ± 2.0
3t	3	6-NO_2	4-Dimethylamine	22.9 ± 0.7	38.3 ± 0.9	45.3 ± 0.7	53.6 ± 0.7	56.3 ± 1.6	68.2 ± 0.1	71.8 ± 1.1
Quercetin	—	—	—	28.0 ± 0.8	37.7 ± 1.2	44.2 ± 0.7	50.7 ± 0.1	55.8 ± 0.3	59.6 ± 0.8	61.0 ± 0.8

[a]*Cell viability was determined using the MTT assay protocol. Data are expressed as the mean ± SEM of three independent replicates.*

2.2.4 Cytotoxicity and Neuroprotection Against $A\beta_{1-42}$-Induced Cytotoxicity in SH-SY5Y Cells

The cytotoxic effects of the best neuroprotective compounds **3a**, **3f,** and **3t** at a concentration of 1 μM were also evaluated on SH-SY5Y cells (**Table 3**). The results showed that all three compounds showed no cytotoxic effect on SH-SY5Y cells. Additionally, the potential neuroprotective effect of compounds **3a**, **3f,** and **3t** against $A\beta_{1-42}$-induced cytotoxicity in SH-SY5Y cells was evaluated at a concentration of 1 μM. Compounds **3a** and **3f** could increase cell viability in the presence of Aβ and protect neuronal cells against Aβ toxic effects (**Table 4**). However, compound **3t** could not protect

TABLE 3 | The cytotoxic effect of selected compounds **3a**, **3f,** and **3t** on the SH-SY5Y cell line.

Compound	n	R	R′	SH-SY5Y cell viability (% of control)[a]
				1 μM
3a	3	H	H	81.2 ± 10.0
3f	3	6-NO_2	H	83.6 ± 3.4
3t	3	6-NO_2	H	84.8 ± 6.8

[a]*Cell viability is expressed as the mean percentage of viable cells compared with the untreated cells using the MTT assay protocol. The data are the mean ± SEM.*

TABLE 4 | The protective effect of compounds **3a**, **3f,** and **3t** against amyloid-induced injury in the SH-SY5Y cell line in comparison to Donepezil[a].

Compound	n	R	R′	SH-SY5Y cell viability (% of control)
				1 μM
3a	3	H	H	79.1 ± 4.0
3f	3	6-NO_2	H	89.0 ± 9.8
3t	3	6-NO_2	H	59.7 ± 2.8
Donepezil	—	—	—	77.1 ± 3.6
$A\beta_{1\text{-}42}$	—	—	—	72.2 ± 7.5

[a]*Protective effects of compounds **3a**, **3f** and **3t** on cell injury induced by $A\beta_{1\text{-}42}$ in SH-SY5Ycells. All groups were treated with 5 μM $A\beta_{1\text{-}42}$ except for the control group. The synthetic compounds and Donepezil were pre-incubated at 1 μm of concentration in serum-free media for 24 h before the addition of Aβ peptide. Cell viability is expressed as the mean percentage of viable cells compared with the untreated cells. The data are the mean ± SEM.*

TABLE 5 | Inhibition of Aβ self- and AChE-induced aggregation by the compounds **3a**, **3f,** and **3t**.

Compound	Inhibition of self-induced Aβ aggregation[a](%)	Inhibition of AChE-induced Aβ aggregation[b](%)
3a	73.3 ± 15.4	76.0 ± 1.6
3f	84.7 ± 1.6	87.2 ± 5.7
3t	66.4 ± 4.7	52.5 ± 4.9
Donepezil	30.8 ± 1.7	71.9 ± 1.2

[a]*Inhibition of self-induced $A\beta_{1\text{-}42}$ aggregation (20 μM) produced by the tested compound at 100 μM concentration after 48 h. Values are expressed as means ± SEM of three experiments.*

[b]*Co-aggregation inhibition of $A\beta_{1\text{-}42}$ and AChE (0.01 u/ml) by the tested compound at 100 μM concentration was detected by ThT assay. Values are expressed as means ± SEM of three experiments.*

neuronal cells at a concentration of 1 μM. According to the results, compounds **3a** and **3f** showed protective capability with acceptable cell viability of 79% and 89%, respectively, at concentrations of 1 μM, higher than donepezil as the reference drug (77%).

2.2.5 Inhibitory Potency of the Compounds Against Self-Induced and AChE-Induced $A\beta_{1\text{-}42}$ Aggregation

The potential of compounds **3a**, **3f,** and **3t**, as the most active compounds based on the performed analyses, to inhibit Aβ-aggregation was evaluated using the thioflavin T (ThT) assay. The results indicated that the tested compounds displayed inhibitory activity about 2-fold more effective than the reference drug donepezil against Aβ aggregation (30.8% inhibition for donepezil vs. 73.3%, 84.7%, and 66.4% inhibition for compounds **3a**, **3f,** and **3t**, respectively, **Table 5**). The potential of compounds **3a**, **3f,** and **3t** to inhibit Aβ aggregation induced by AChE was also evaluated (**Table 5**). Compounds **3a**, **3f,** showed good inhibition activity toward AChE-induced Aβ aggregation (76.0% and 87.2% inhibition, respectively) more than donepezil as the standard drug (71.9% inhibition), except for compound **3t,** which was less active (52.5% inhibition) than donepezil. Compound **3f,** as the most active BuChE inhibitor, exhibited the most inhibition activity against both self and AChE-indued Aβ aggregation (84.7% and 87.2% inhibition, respectively).

3 CONCLUSION

In this work, coumarin derivatives were cross-linked to pyridinium salts via flexible aliphatic carbon chains, and the target compounds were evaluated as MTDLs against AD. All the compounds showed high AChE and BuChE inhibition activity in the nano-molar range. Compound **3f** exhibited 7 times more AChE inhibition activity and compound **3t** had a 305 times greater inhibitory effect against BuChE compared to the standard drug. Especially, compound **3f** as the best AChE inhibitor (IC_{50} = 2 nM) with acceptable BuChE inhibition activity (IC_{50} = 24 nM, more than 100 times more active than the standard drug), represented an additional advantage through reducing β-amyloid self and AChE-induced aggregation more active than the standard drug and also revealed higher neuroprotective activity against H_2O_2-induced cell death in PC12 cells and against amyloid toxic effects in SH-SY5Y cells than the reference drugs. All the results suggest that the new designed hybrids of coumarin and pyridinium parts could be considered as promising multifunctional agents for further developments in the field of anti-Alzheimer drugs.

4 EXPERIMENTAL

4.1 Chemistry

All commercially available chemicals were purchased from Merck, Sigma, and across without further purification. FT-IR spectra were run on a Bruker Equinox 55 spectrometer. ^{1}H NMR and ^{13}C NMR were recorded on Brucker 400 MHz instrument with frequencies of 400 and 100 MHz, respectively. DMSO was used as a solvent for NMR analyses and tetramethylsilane was employed as an internal standard. The chemical shifts (δ) and coupling constants (*J*) were expressed in parts per million and Hertz, respectively. Melting points were measured by the Buchi melting point B-540 B.V.CHI device. Analytical thin-layer chromatography (TLC) was performed on aluminum plates precoated with silica gel 60F-254 as the adsorbent. Mass spectra were obtained by HP Agilent Technologies 5973 at ionization potential of 70 eV. Elemental analyses were performed with CHNS-varioEL.

4.1.1 General Procedure for the Synthesis of Compound 1

The coumarin derivatives (**1a–f**) were synthesized via the Perkin–Oglialoro reaction according to the previously reported procedure (Abdshahzadeh et al., 2019). A solution containing anhydrous NaOAc (2 mmol), 4-Hydroxyphenylacetic acid (1 mmol), and salicylaldehyde (1 mmol) in Ac_2O (1 ml) was refluxed for 2 h. After completion of the reaction, the mixture was cooled, neutralized with an aqueous $NaHCO_3$ solution, filtered, and washed with distilled water. The compounds were used in the next step without further purification.

4.1.2 General Procedure for the Synthesis of Intermediate 2

Preparation of intermediate **2** was carried out according to the previously reported method (Hirbod et al., 2017). In brief, to a solution of 3-arylcoumarin (1 mmol) and anhydrous K_2CO_3 (2 mmol) in acetone (3 ml), corresponding dibromoalkane (10 mmol) was added and the solution was refluxed for 4 h until the starting material disappeared (monitored by TLC). The solvent was removed under vacuum, hexane was added to the residue, and the product was filtered off and used in the next step without further purification.

4.1.3 General Procedure for the Synthesis of Compounds 3a–q

To a solution containing compound **2** (0.25 mmol), the pyridine derivative (3.1 ml) was added. The mixture was stirred at 80°C for 24 h. The completion of the reaction was monitored by TLC. The mixture was cooled to room temperature, diethyl ether (10 ml) was added, and the mixture was cooled in the refrigerator for 2 h. The obtained solid was finally filtered and dried to obtain **3a–q**.

4.1.3.1 1-(3-(4-(2-Oxo-2H-chromen-3-yl)phenoxy)propyl) pyridinium Bromide 3a

Yield 91%; White solid; m.p. 280–282°C; FT-IR (ATR, cm^{-1}) υ_{max}: 3417, 2943, 1718, 1606, 1511, 1250, 1182, 1099, and 772; ^{1}H NMR (400 MHz, DMSO-d_6)/δ ppm: 9.18 (d, J = 4.0 Hz, 2H), 8.64 (t, J = 5.2 Hz, 1H), 8.18–8.19 (m, 3H), 7.77 (d, J = 5.6 Hz, 1H), 7.67 (d, J = 6.0 Hz, 2H), 7.59 (t, J = 5.6 Hz, 1H), 7.42 (d, J = 6.4 Hz, 1H), 7.38 (t, J = 5.2 Hz, 1H), 6.87 (d, J = 6.0 Hz, 2H), 4.84 (t, J = 4.0 Hz, 2H), 4.15 (t, J = 4.0 Hz, 2H), 2.35 (m, 2H); ^{13}C NMR (100 MHz, DMSO-d_6)/δ ppm: 159.8, 158.2, 152.7, 145.6, 145.1, 139.2, 131.4, 128.4, 127.9, 127.2, 126.3, 124.6, 119.6, 115.8, 114.0, 65.0, 58.9, 29.9; MS m/z: 438.3 (M^+), 278.1 ($C_{18}H_{15}O_3^{\bullet}$), 238.1 ($C_{15}H_9O_3^{\bullet}$), 79.1 ($C_5H_5N^{\bullet+}$); Anal. Calcd. for $C_{23}H_{20}BrNO_3$ (438.31): C, 63.02; H, 4.60; N, 3.20. Found: C, 62.96; H, 4.71; N, 3.00.

4.1.3.2 1-(3-(4-(6-Methoxy-2-oxo-2H-chromen-3-yl) phenoxy)propyl)pyridinium Bromide 3b

Yield 94%; White solid; m.p. 196–198°C; FT-IR (ATR cm^{-1}) υ_{max}: 3417, 3025, 1706, 1605, 1576, 1248, 1112, 1050, 771; ^{1}H NMR (400 MHz, DMSO-d_6)/δ ppm: 9.18 (d, J = 4.8 Hz, 2H), 8.64 (t, J = 5.2 Hz, 1H), 8.14–8.21 (m, 3H), 7.65 (d, J = 6.8 Hz, 2H), 7.36 (d, J = 7.2 Hz, 1H), 7.32 (s, 1H), 7.18 (d, J = 5.2 Hz, 1H), 6.87 (d, J = 6.8 Hz, 2H), 4.84 (t, J = 5.2 Hz, 2H), 4.15 (t, J = 4.0 Hz, 2H), 3.81 (s, OCH_3, 3H), 2.20 (m, 2H); ^{13}C NMR (100 MHz, DMSO-d_6)/δ ppm: 159.9, 158.2, 155.6, 147.1, 145.1, 139.1, 129.8, 128.2, 127.9, 127.2, 126.5, 120.0, 118.8, 116.9, 114.2, 114.0, 110.6, 65.0, 58.9, 55.7, 29.9; MS m/z: 468.3 (M+), 388.1 ($C_{24}H_{22}NO_4^{2\bullet+}$), 268.1 ($C_{16}H_{11}O_4^{\bullet}$), 139.1 ($C_8H_{11}NO^{\bullet+}$), 79.1 ($C_5H_5N^{\bullet+}$); Anal. Calcd. for $C_{24}H_{22}BrNO_4$ (468.34): C, 61.55; H, 4.73; N, 2.99. Found: C, 61.34; H, 4.81; N, 2.97.

4.1.3.3 1-(3-(4-(7-Methoxy-2-oxo-2H-chromen-3-yl) phenoxy)propyl)pyridinium Bromide 3c

Yield 88%; Cream solid; m.p. 256–258°C; FT-IR (ATR cm^{-1}) υ_{max}: 3466, 3017, 1714, 1604, 1510, 1250, 1118, 1049, 771; ^{1}H NMR (400 MHz, DMSO-d_6)/δ ppm: 9.17 (d, J = 4.4 Hz, 2H), 8.63 (t, J = 6.4 Hz, 1H), 8.13–8.17 (m, 3H), 7.64 (m, 3H), 6.97–7.02 (m, 2H), 6.84 (m, 2H), 4.84 (t, J = 4.0 Hz, 2H), 4.14 (t, J = 4.0 Hz, 2H), 3.86 (s, OCH_3, 3H), 2.34 (m, 2H); ^{13}C NMR (100 MHz, DMSO-d_6)/δ ppm: 162.4, 160.1, 157.9, 154.5, 145.6, 145.3, 144.9, 129.7, 129.4, 128.0, 127.9, 127.4, 113.9, 113.1, 100.1, 95.1, 65.3, 58.9, 56.4, 26.7.

4.1.3.4 1-(3-(4-(8-Methoxy-2-oxo-2H-chromen-3-yl) phenoxy)propyl)pyridinium Bromide 3d

Yield 89%; Cream solid; m.p. 209–211°C; FT-IR (ATR cm^{-1}) υ_{max}: 3419, 3013, 1719, 1606, 1510, 1249, 1177, 1095, 772; ^{1}H NMR (400 MHz, DMSO-d_6)/δ ppm: 9.18 (d, J = 4.8 Hz, 2H), 8.63 (t, J = 4.0 Hz, 1H), 8.17–8.21 (m, 3H), 7.67 (d, J = 6.8 Hz, 2H), 7.28–7.31 (m, 3H), 6.86 (d, J = 6.8 Hz, 2H), 4.46 (t, J = 4.0 Hz, 2H), 4.10 (t, J = 4.0 Hz, 2H), 3.92 (s, OCH_3, 3H), 2.25 (m, 2H); ^{13}C NMR (100 MHz, DMSO-d_6)/δ ppm: 159.5, 158.2, 146.2, 145.1, 145.0, 142.0, 139.4, 129.8, 127.9, 127.1, 126.3, 124.5, 120.1, 119.7, 114.0, 113.6, 65.0, 58.9, 56.1, 29.9.

4.1.3.5 1-(3-(4-(6-Bromo-2-oxo-2H-chromen-3-yl)phenoxy) propyl)pyridinium Bromide 3e

Yield 94%; White solid; m.p. 232–234°C; FT-IR (ATR cm^{-1}) υ_{max}: 3445, 3018, 1719, 1606, 1511, 1251, 1098, 770; ^{1}H NMR (400 MHz, DMSO-d_6)/δ ppm: 9.20 (d, J = 5.6 Hz, 2H), 8.66 (t, J = 7.6 Hz, 1H), 8.17–8.22 (m, 3H), 8.03 (s, 1H), 7.77 (d, J = 7.6 Hz, 1H), 7.68 (d, J = 8.4 Hz, 2H), 7.43 (d, J = 8.8 Hz, 1H), 6.91 (d, J = 8.4 Hz, 2H), 4.86 (t, J = 6.4 Hz, 2H), 4.18 (t, J = 6.4 Hz, 2H), 2.52 (m, 2H); ^{13}C NMR (100 MHz, DMSO-d_6)/δ ppm: 159.8, 158.9, 152.2, 146.1, 145.5, 138.3, 134.1, 130.8, 130.3, 128.4, 127.8, 127.3, 122.0, 118.6, 116.5, 114.6, 65.5, 59.4, 30.3.

4.1.3.6 1-(3-(4-(6-Nitro-2-oxo-2H-chromen-3-yl)phenoxy) propyl)pyridinium Bromide 3f

Yield 93%; Cream solid; m.p. 240–243°C; FT-IR (ATR cm^{-1}) υ_{max}: 3444, 3011, 1742, 1607, 1510, 1231, 769; ^{1}H NMR (400 MHz, DMSO-d_6)/δ ppm: 9.18 (d, J = 4.4 Hz, 2H), 8.74 (s, 1H), 8.63 (t, J = 6.0 Hz, 1H), 8.36–8.41 (m, 2H), 8.18 (t, J = 5.2 Hz, 2H), 7.64–7.68 (m, 3H), 6.89 (d, J = 6.8 Hz, 2H), 4.83 (t, J = 5.2 Hz, 2H), 4.16 (t, J = 4.0 Hz, 2H), 2.22 (m, 2H); ^{13}C NMR (100 MHz, DMSO-d_6)/δ ppm: 159.5, 158.9, 158.6, 156.3, 145.6, 145.1, 143.6, 129.9, 128.0, 128.0, 126.4, 125.8, 120.0, 117.3, 114.1, 65.0, 58.9, 29.9; MS m/z: 483.3 (M^+), 323.2 ($C_{18}H_{14}NO_5^{\bullet}$), 282.1 ($C_{15}H_8NO_5^{\bullet}$), 79.2 ($C_5H_5N^{\bullet+}$); Anal. Calcd. for $C_{23}H_{19}BrN_2O_5$

(483.31): C, 57.16; H, 3.96; N, 5.80. Found: C, 57.01; H, 3.98; N, 5.71.

4.1.3.7 1-(4-(4-(2-Oxo-2H-chromen-3-yl)phenoxy)butyl) pyridinium Bromide 3g

Yield 93%; Pale yellow solid; m.p. 180–185°C; FT-IR (ATR cm^{-1}) υ_{max}: 3413, 3013, 1708, 1607, 1510, 1250, 1176, 1098, 773; ^1H NMR (400 MHz, DMSO-d_6)/δ ppm: 9.17 (d, J = 4.4 Hz, 2H), 8.63 (t, J = 6.0 Hz, 1H), 8.18–8.20 (m, 3H), 7.77 (d, J = 6.0 Hz, 1H), 7.69 (d, J = 6.8 Hz, 2H), 7.59 (t, J = 6.0 Hz, 1H), 7.42 (d, J = 6.4 Hz, 1H), 7.37 (t, J = 5.6 Hz, 1H), 7.01 (d, J = 6.8 Hz, 2H), 4.72 (t, J = 6.0 Hz, 2H), 4.07 (t, J = 4.4 Hz, 2H), 2.09–2.12 (m, 2H), 1.75–1.77 (m, 2H). ^{13}C NMR (100 MHz, DMSO-d_6)/δ ppm: 159.9, 158.7, 152.7, 145.5, 144.8, 139.1, 131.3, 129.8, 128.4, 128.1, 126.9, 126.3, 124.6, 119.6, 115.8, 114.2, 66.8, 60.4, 27.7, 25.2; MS m/z: 452.3 (M^+), 238.1 ($C_{15}H_9O_3^{\bullet}$), 135.1 ($C_9H_{13}N^{\bullet+}$), 79.1 ($C_5H_5N^{\bullet+}$), 55.1 ($C_4H_8^{2\bullet}$); Anal. Calcd. for $C_{24}H_{22}BrNO_3$ (452.34): C, 63.73; H, 4.90; N, 3.10. Found: C, 63.59; H, 4.98; N, 2.95.

4.1.3.8 1-(4-(4-(6-Methoxy-2-oxo-2H-chromen-3-yl) phenoxy)butyl)pyridinium Bromide 3h

Yield 92%; Cream solid; m.p. 189–192°C; FT-IR (ATR cm^{-1}) υ_{max}: 3444, 2946, 1710, 1606, 1578, 1254, 1104, 1023, 770; ^1H NMR (400 MHz, DMSO-d_6)/δ ppm: 9.14 (d, J = 4.0 Hz, 2H), 8.61 (t, J = 5.6 Hz, 1H), 8.14–8.18 (m, 3H), 7.67 (d, J = 6.4 Hz, 2H), 7.37 (d, J = 6.8 Hz, 1H), 7.31 (s, 1H), 7.19 (d, J = 6.4 Hz, 1H), 7.01 (d, J = 6.4 Hz, 2H), 4.70 (t, J = 5.6 Hz, 2H), 4.07 (t, J = 4.0 Hz, 2H), 3.81 (s, OCH_3, 3H), 2.1 (m, 2H), 1.77 (m, 2H); ^{13}C NMR (100 MHz, DMSO-d_6)/δ ppm: 159.8, 158.6, 155.6, 148.1, 144.9, 144.4, 142.1, 139.2, 129.8, 128.1, 126.5, 119.9, 118.2, 116.9, 114.2, 110.4, 66.8, 60.7, 55.6, 27.5, 25.0.

4.1.3.9 1-(4-(4-(7-Methoxy-2-oxo-2H-chromen-3-yl) phenoxy)butyl)pyridinium Bromide 3i

Yield 90%; Brown solid; m.p. 186–188°C; FT-IR (ATR cm^{-1}) υ_{max}: 3479, 3013, 1719, 1606, 1510, 1250, 1117, 1096, and 773; ^1H NMR (400 MHz, DMSO-d_6)/δ ppm: 9.16 (d, J = 4.0 Hz, 2H), 8.62 (t, J = 8.0 Hz, 1H), 8.14–8.18 (m, 3H), 7.67 (m, 3H), 6.98–7.01 (m, 4H), 4.71 (t, J = 4.0 Hz, 2H), 4.06 (t, J = 4.0 Hz, 2H), 3.86 (s, OCH_3, 3H), 2.11 (m, 2H), and 1.76 (m, 2H); ^{13}C NMR (100 MHz, DMSO-d_6)/δ ppm: 166.05, 162.61, 152.72, 145.59, 144.73, 139.92, 131.39, 129.62, 128.38, 128.08, 126.59, 126.35, 123.07, 119.97, 114.22, 112.41, 66.84, 60.81, 55.67, 55.35, 27.48, 25.44.

4.1.3.10 1-(4-(4-(8-Methoxy-2-oxo-2H-chromen-3-yl) phenoxy)butyl)pyridinium Bromide 3j

Yield 90%; Pale yellow solid; m.p. 105–107°C; FT-IR (ATR cm^{-1}) υ_{max}: 3416, 3012, 2940, 1719, 1606, 1574, 1276, 1177, 1095, and 773; ^1H NMR (400 MHz, DMSO-d_6)/δ ppm: 9.17 (d, J = 4.0 Hz, 2H), 8.62 (t, J = 6.0 Hz, 1H), 8.17 (m, 3H), 7.68–7.70 (m, 2H), 7.28–7.30 (m, 3H), 7.00 (d, J = 6.4 Hz, 2H), 4.70 (t, J = 5.2 Hz, 2H), 4.06 (t, J = 4.0 Hz, 2H), 3.91 (s, OCH_3, 3H), 2.11 (m, 2H), and 1.76 (m, 2H); ^{13}C NMR (100 MHz, DMSO-d_6)/δ ppm: 159.6, 158.7, 146.2, 146.2, 145.5, 144.6, 141.9, 139.2, 129.9, 129.6, 128.2, 126.8, 120.4, 124.5, 120.1, 114.2, 66.8, 60.4, 55.9, 27.7, 25.2.

4.1.3.11 1-(4-(4-(6-Bromo-2-oxo-2H-chromen-3-yl)phenoxy) butyl)pyridinium Bromide 3k

Yield 94%; Cream solid; m.p. 256–258°C; FT-IR (ATR cm^{-1}) υ_{max}: 3412, 2943, 1727, 1606, 1511, 1251, 1182, 1098, and 774; ^1H NMR (400 MHz, DMSO-d_6)/δ ppm: 9.21 (d, J = 5.2 Hz, 2H), 8.65 (t, J = 7.6 Hz, 1H), 8.18–8.23 (m, 3H), 8.03 (s, 1H), 7.75 (d, J = 8.8 Hz, 1H), 7.69 (d, J = 8.4 Hz, 2H), 7.41 (d, J = 8.8 Hz, 1H), 7.04 (d, J = 8.4 Hz, 2H), 4.75 (t, J = 7.2 Hz, 2H), 4.10 (t, J = 6.0 Hz, 2H), 2.10–2.15 (m, 2H), and 1.77–1.81 (m, 2H); ^{13}C NMR (100 MHz, DMSO-d_6)/δ ppm: 159.8, 158.4, 152.2, 146.0, 145.3, 138.1, 134.0, 130.8, 130.3, 128.6, 127.8, 127.0, 122.0, 118.5, 116.5, 114.7, 67.4, 60.9, 28.2, 25.6.

4.1.3.12 1-(4-(4-(6-Nitro-2-oxo-2H-chromen-3-yl)phenoxy) butyl)pyridinium Bromide 3l

Yield 93%; Yellow solid; m.p. 223–226°C; FT-IR (ATR cm^{-1}) υ_{max}: 3407, 2943, 1724, 1607, 1513, 1252, 1182, 1095, and 773; ^1H NMR (400 MHz, DMSO-d_6)/δ ppm: 9.17 (d, J = 4.4 Hz, 2H), 8.74 (s, 1H), 8.62 (t, J = 6.0 Hz, 1H), 8.37–8.39 (m, 2H), 8.19 (t, J = 5.6 Hz, 2H), 7.69 (d, J = 6.8 Hz, 2H), 7.64 (d, J = 7.2 Hz, 1H), 7.04 (d, J = 6.8 Hz, 2H), 4.72 (t, J = 5.6 Hz, 2H), 4.08 (t, J = 4.8 Hz, 2H), 2.10–2.13 (m, 2H), and 1.75–1.78 (m, 2H); ^{13}C NMR (100 MHz, DMSO-d_6)/δ ppm: 159.1, 158.9, 156.3, 145.5, 144.8, 143.5, 137.8, 129.9, 128.1, 128.0, 126.4, 126.1, 125.8, 124.1, 120.0, 117.3, 114.3, 66.9, 60.4, and 27.7, 25.2; MS m/z: 497.3 (M^+), 283.1 ($C_{15}H_8NO_5^{\bullet}$), 135.1 ($C_9H_{13}N^{\bullet+}$), 55.2 ($C_4H_8^{2\bullet}$); Anal. Calcd. for $C_{24}H_{21}BrN_2O_5$ (497.34): C, 57.96; H, 4.26; N, 5.63. Found: C, 57.73; H, 4.35; N, 5.58.

4.1.3.13 1-(5-(4-(2-Oxo-2H-chromen-3-yl)phenoxy)pentyl) pyridinium Bromide 3m

Yield 94%; White solid; m.p. 100–103°C; FT-IR (ATR cm^{-1}) υ_{max}: 3443, 2943, 1695, 1606, 1512, 1280, 1124, 1050, and 766; ^1H NMR (400 MHz, DMSO-d_6)/δ ppm: 9.12 (d, J = 4.4 Hz, 2H), 8.62 (t, J = 6.0 Hz, 1H), 8.16–8.19 (m, 3H), 7.77 (d, J = 6.0 Hz, 1H), 7.69 (d, J = 6.8 Hz, 2H), 7.60 (t, J = 6.0 Hz, 1H), 7.42 (d, J = 6.4 Hz, 1H), 7.37 (t, J = 6.0 Hz, 1H), 7.00 (d, J = 6.8 Hz, 2H), 4.64 (t, J = 6.0 Hz, 2H), 4.03 (t, J = 4.8 Hz, 2H), 2.00–2.02 (m, 2H), 1.77–1.80 (m, 2H), 1.43–1.46 (m, 2H); ^{13}C NMR (100 MHz, DMSO-d_6)/δ ppm: 158.9, 158.7, 152.7, 145.5, 144.8, 138.8, 131.3, 129.8, 128.4, 128.1, 126.9, 126.3, 124.6, 119.6, 115.8, 114.2, 66.8, 60.6, 30.4, 28.6, 22.0.

4.1.3.14 1-(5-(4-(8-Methoxy-2-oxo-2H-chromen-3-yl) phenoxy)pentyl)pyridinium Bromide 3n

Yield 92%; Cream solid; m.p. 234–235°C; FT-IR (ATR cm^{-1}) υ_{max}: 3357, 2941, 1697, 1606, 1278, 1098, 1050, 775; ^1H NMR (400 MHz, DMSO-d_6)/δ ppm: 9.14 (d, J = 4.4 Hz, 2H), 8.62 (t, J = 6.0 Hz, 1H), 8.16–8.19 (m, 3H), 7.70 (d, J = 6.8 Hz, 2H), 7.28–7.31 (m, 3H), 6.98 (d, J = 6.8 Hz, 2H), 4.66 (t, J = 5.6 Hz, 2H), 4.03 (t, J = 4.8 Hz, 2H), 3.92 (s, OCH_3, 3H), 1.99–2.02 (m, 2H), 1.77–1.80 (m, 2H), and 1.45–1.46 (m, 2H); ^{13}C NMR (100 MHz, DMSO-d_6)/δ ppm: 159.6, 158.9, 146.2, 145.5, 144.8, 141.9, 139.2, 129.8, 128.1, 126.7, 126.4, 124.5, 120.1, 119.6, 114.1, 113.5, 67.1, 60.6, 56.0, 30.4, 27.9, 22.0.

4.1.3.15 1-(5-(4-(6-Nitro-2-oxo-2H-chromen-3-yl)phenoxy) pentyl)pyridinium Bromide 3o

Yield 91%; Pale yellow solid; m.p. 286–288°C; FT-IR (ATR cm^{-1}) υ_{max}: 3419, 2944, 1730, 1607, 1512, 1250, 1096, 769; ^{1}H NMR (400 MHz, DMSO-d_6)/δ ppm: 9.13 (d, *J* = 4.4 Hz, 2H), 8.74 (s, 1H), 8.62 (t, *J* = 6.0 Hz, 1H), 8.38–8.40 (m, 2H), 8.18 (t, *J* = 5.6 Hz, 2H), 7.69 (d, *J* = 6.8 Hz, 2H), 7.64 (d, *J* = 7.2 Hz, 1H), 7.03 (d, *J* = 6.8 Hz, 2H), 4.66 (t, *J* = 6.0 Hz, 2H), 4.04 (t, *J* = 5.2 Hz, 2H), 2.00–2.04 (m, 2H), 1.76–1.81 (m, 2H), 1.42–1.48 (m, 2H); ^{13}C NMR (100 MHz, DMSO-d_6)/δ ppm: 159.3, 158.9, 156.13, 145.5, 144.8, 143.5, 137.7, 129.9, 128.1, 126.0, 125.7, 124.1, 120.0, 117.3, 114.3, 67.2, 60.5, 30.4, 27.9, 22.0.

4.1.3.16 1-(5-(4-(6-Bromo-2-oxo-2H-chromen-3-yl)phenoxy) pentyl)pyridinium Bromide 3p

Yield 95%; Cream solid; m.p. 240–242°C; FT-IR (ATR cm^{-1}) υ_{max}: 3449, 2944, 1711, 1605, 1508, 1283, 1113, and 771; ^{1}H NMR (400 MHz, DMSO-d_6)/δ ppm: 9.21 (d, *J* = 5.6 Hz, 2H), 8.65 (t, *J* = 7.6 Hz, 1H), 8.19–8.22 (m, 3H), 8.02 (s, 1H), 7.75 (d, *J* = 8.4 Hz, 1H), 7.69 (d, *J* = 8.0 Hz, 2H), 7.41 (d, *J* = 8.8 Hz, 1H), 7.04 (d, *J* = 8.0 Hz, 2H), 4.71 (t, *J* = 6.8 Hz, 2H), 4.03 (t, *J* = 6.0 Hz, 2H), 2.01–2.09 (m, 2H), 1.78–1.81 (m, 2H), 1.45–1.48 (m, 2H); ^{13}C NMR (100 MHz, DMSO-d_6)/δ ppm: 159.8, 158.4, 152.2, 146.0, 145.3, 138.1, 134.0, 130.8, 130.3, 128.6, 127.8, 127.0, 122.0, 118.5, 116.5, 114.7, 67.4, 60.9, 30.9, 28.2, 25.6.

4.1.3.17 1-(5-(4-(6-Bromo-2-oxo-2H-chromen-3-yl)phenoxy) pentyl)-5-ethyl-2-methylpyridin-1-ium Bromide 3q

Yield 54%; Yellow oil; FT-IR (KBr cm^{-1}) υ_{max}: 3394, 2921, 1720, 1613, 1530, 1467, 1252, 1112, 828; ^{1}H NMR (400 MHz, DMSO-d_6)/δ ppm: 8.98 (s, 1H), 8.40 (d, *J* = 8.8 Hz, 1H), 8.18 (s, 1H), 8.04 (d, *J* = 2.4 Hz, 1H), 7.99 (d, *J* = 8.4 Hz, 1H), 7.76 (d, *J* = 6.8 Hz,1H), 7.70 (d, *J* = 8.8 Hz, 2H), 7.42 (d, *J* = 8.8 Hz, 1H), 7.04 (d, *J* = 8.8 Hz, 2H), 4.57 (t, *J* = 7.6 Hz, 2H), 4.08 (t, *J* = 6.4 Hz, 2H), 2.82 (s, 3H), 2.78–2.80 (m, 2H), 1.85–1.96 (m, 2H), and 1.25–1.28 (m, 4H); 1.04–1.06 (m, 3H); ^{13}C NMR (100 MHz, DMSO-d_6)/δ ppm: 159.8, 158.4, 152.2, 146.0, 145.3, 138.1, 134.0, 130.8, 130.3, 128.6, 127.8, 127.0, 122.0, 118.5, 116.5, 114.7, 67.4, 60.9, 30.9, 28.2, and 25.6; ^{13}C NMR (100 MHz, DMSO-d_6)/δ ppm: 159.9, 159.6, 152.8, 152.2, 145.1, 144.6, 142.0, 138.1, 134.0, 130.8, 130.3, 129.9, 127.9, 126.9, 122.0, 118.6, 116.5, 114.7, 67.7, 57.5, 29.6, 28.5, 25.1, 22.9, 19.5, 14.8.

4.1.4 General Procedure for the Synthesis of Compound 3r–t

A mixture of compound **2** (1 mmol) and 4-dimethylaminopyridine (1.5 mmol) in dry acetonitrile (5 ml) was stirred at 70°C for 24 h. After completion of the reaction (monitored by TLC), the mixture was cooled to room temperature and acetone (20 ml) was then added. The mixture was cooled in the refrigerator (5°C) overnight. The solid was filtered and crystalized using acetone.

4.1.4.1 4-(Dimethylamino)-1-(3-(4-(6-bromo-2-oxo-2H-chromen-3-yl)phenoxy)pentyl) pyridin-1-ium Bromide 3r

Yield 65%; Yellow solid; m.p. 146–148°C; FT-IR (ATR, cm^{-1}) υ_{max}: 3375, 3067, 2942, 1716, 1649, 1606, 1565, 1472, 1255, 1179, 1066, and 825; ^{1}H NMR (400 MHz, DMSO-d_6)/δ ppm: 8.41 (d, *J* = 7.2 Hz, 2H), 8.19 (s, 1H), 8.02 (s, 1H), 7.73 (d, *J* = 1.6 Hz, 1H), 7.69 (d, *J* = 8.4 Hz, 2H), 7.38 (d, *J* = 8.8 Hz,1H), 7.06 (d, *J* = 7.2 Hz, 2H), 7.00 (d, *J* = 8.4 Hz, 2H), 4.26 (t, *J* = 6.8 Hz, 2H), 4.02 (t, *J* = 6.0 Hz, 2H), 3.83 (s, 6H), 1.84–1.87 (m, 2H), 1.76–1.81 (m, 2H), and 1.41–1.42 (m, 2H); ^{13}C NMR (100 MHz, DMSO-d_6)/δ ppm: 159.8, 159.5, 158.4, 156.2, 152.1, 142.5, 138.1, 134.0, 130.8, 130.3, 127.7, 126.8, 122.0, 118.5, 116.5, 114.6, 108.1, 67.7, 56.9, 30.5, 28.4, 22.5.

4.1.4.2 4-(Dimethylamino)-1-(3-(4-(2-oxo-2H-chromen-3-yl) phenoxy)propyl)pyridin-1-ium Bromide 3s

Yield 60%; White solid; m.p. 233–235°C; FT-IR (ATR cm^{-1}) υ_{max}: 3370, 3057, 2883, 1715, 1645, 1607, 1568, 1509, 1255, 1177, 1115, 768; ^{1}H NMR (400 MHz, DMSO-d_6)/δ ppm: 8.43 (d, *J* = 7.6 Hz, 2H), 8.23 (s, 1H), 7.80 (d, *J* = 7.6 Hz, 1H), 7.70 (d, *J* = 8.8 Hz, 2H), 7.61 (t, *J* = 7.6 Hz,1H), 7.42 (d, *J* = 8.4 Hz, 1H), 7.37 (d, *J* = 7.6 Hz, 1H), 7.06 (d, *J* = 7.2 Hz, 2H), 6.98 (d, *J* = 8.8 Hz, 2H), 4.43 (t, *J* = 6.4 Hz, 2H), 4.08 (t, *J* = 5.6 Hz, 2H), 3.20 (s, 6H), 2.29–2.32 (m, 2H); ^{13}C NMR (100 MHz, DMSO-d_6)/δ ppm: 160.3, 158.9, 156.3, 153.1, 142.7, 139.7, 131.8, 130.3, 128.9, 127.5, 126.7, 125.0, 120.0, 116.2, 114.6, 108.1, 65.1, 54.7, 40.2, 30.1. MS m/z: 481.3 (M^+), 388.1 ($C_{24}H_{22}N_2O_3^{\bullet+}$), 238.1 ($C_{15}H_9O_3^{\bullet}$), 121.2 ($C_7H_{10}N_2^{\bullet+}$); Anal. Calcd. for $C_{25}H_{25}BrN_2O_3$ (481.38): C, 62.38; H, 5.23; N, 5.82; O, 9.97. Found: C, 62.25; H, 5.42; N, 5.77.

4.1.4.3 4-(Dimethylamino)-1-(3-(4-(6-nitro-2-oxo-2H-chromen-3-yl)phenoxy)propyl) pyridin-1-ium Bromide 3t

Yield 72%; Yellow solid; m.p. 173–174°C; FT-IR (ATR cm^{-1}) υ_{max}: 3365, 1722, 1649, 1611, 1564, 1517, 1343, 1255, 1176, 1095, 942, 825; ^{1}H NMR (400 MHz, DMSO-d_6)/δ ppm: 8.76 (d, *J* = 2.8 Hz, 1H), 8.43 (d, *J* = 2.4 Hz, 1H), 8.40 (s, 1H), 8.37 (d, *J* = 7.2 Hz, 2H), 7.72 (d, *J* = 8.8 Hz,2H), 7.68 (d, *J* = 8.8 Hz, 1H), 7.11 (d, *J* = 7.6 Hz, 2H), 7.02 (d, *J* = 8.8 Hz, 2H), 4.41 (t, *J* = 6.8 Hz, 2H), 4.10 (t, *J* = 5.6 Hz, 2H), 3.21 (s, 6H), 2.30–2.33 (m, 2H); ^{13}C NMR (100 MHz, DMSO-d_6)/δ ppm: 159.4, 159.3, 156.8, 156.3, 144.1, 142.7, 138.3, 130.4, 128.5, 126.9, 126.3, 124.6, 120.5, 117.8, 114.7, 108.1, 65.1, 54.8, 40.2, 30.0.

4.2 Biological Assays

4.2.1 Inhibitory Activity of the Target Compounds Against AChE and BChE

To evaluate the AChE and BuChE inhibitory activities, the Ellman's method was employed (Ellman et al., 1961). AChE, BuChE, 5,5'-dithiobis (2-nitrobenzoic acid) (DTNB), acetyl- and butyrylthiocholine iodides were purchased from Sigma-Aldrich. Five different concentrations of the corresponding compounds in ethanol-DMSO (9:1) were prepared. For assay, the corresponding enzyme (5 IU/ml, in phosphate buffer, pH 8.0 containing 25% v/v of glycerol) was added to a 24-well plate containing PBS, the tested compound in different concentrations, and DTNB (0.01 M). After 3 min of incubation, the substrate solution (acetylthiocholine iodide or butyrylthiocholine iodide, 0.05 M) was added and then incubated for at least 1 min at 25°C. The absorbance was measured at 412 μM using a microplate reader (BioTek Synergy HT). The inhibition curve was obtained by plotting the percentage of enzyme activity (100% for the

reference) versus the logarithm of the tested compound concentration. Results are reported as the mean ± SD for at least three different experiments.

4.2.2 Neuroprotection Assay Against H_2O_2-Induced Cell Death in PC12 Cells

The cell viability was measured using MTT [3-(4,5-dimethylthiazol-2-yl)-2,5-diphenyl tetrazolium bromide] assay (Datki et al., 2003). PC12 cells (from the Iranian Biological Resource Center, IBRC) received different treatments, including no treatment (control), 150 μM H_2O_2 alone, or 150 μM H_2O_2 in combination with 0.1–50 μM of the tested compound. The cells were seeded at 1 × 104 cells/well and incubated at 37oC under a 5% CO_2 atmosphere for 24 h, then treated with the tested compound and incubated for 3 h. Next, the cells were exposed to H_2O_2 for 2 h again. The MTT solution (20 μl, 5 mg/ml) was next replaced with the medium and incubated for 4 h. 100 μl of DMSO was added to dissolve the formazan precipitate. Absorbance was then measured at 570 nm using a multi-mode plate reader (Biotek, Winooski, VT). Cell viability is expressed as a percentage relative to the untreated control.

4.2.3 Inhibition of Self- and AChE-Induced $A\beta_{1-42}$ Aggregation

Inhibitory properties of the compounds on self-induced and AChE-induced aggregation of amyloid-β protein 1–42 was determined using a thioflavin T (ThT)-based fluorescence assay with slight modifications (Levine, 1993). The ThT excitation/emission was measured at 448 nm/490 nm at 48 h using a SpectraMax® Microplate Reader. Amyloid-β protein 1–42 (Sigma A9810) was dissolved in Phosphate Buffer Saline pH 7.4 (PBS, HyClone Thermo Scientific) containing ammonium hydroxide (1%). $A\beta_{1-42}$ (50 μM) was incubated for 24 h at 37°C for prefibrillation.

To determine AChE-induced $A\beta_{1-42}$ aggregation, $A\beta_{1-42}$ (20 μl) ± human recombinant AChE (0.01 u/ml, Sigma C1682) were added to 450 ml of PBS buffer pH 7.4 including 0.15 M NaCl and 20 μM thioflavin T (ThT). The mixture was incubated at 37°C in the absence and presence of the compounds (100 μM) and the fluorescence intensities were determined. Due to the presence of the tested compounds, inhibition of self- or AChE-induced aggregation percent was determined by the following calculation: [100-((IFi/IFo) × 100)] where IFi and IFo are the fluorescence intensities obtained for Aβ ± AChE in the presence and in the absence of inhibitors.

4.2.4 Cytotoxicity and Neuroprotection Assay Against $A\beta_{1-42}$-Induced Cytotoxicity in SH-SY5Y Cells

Cell culture chemicals were purchased from Lonza, HyClone, or Thermo Scientific. Human neuroblastoma SH-SY5Y cells were maintained in Dulbecco's modified Eagle's medium (DMEM) supplemented with 10% FBS, 1% L-glutamine, and 1% antibiotic mix at 37°C in a humidified atmosphere containing 5% CO_2. Cell viability was determined using a thiazolyl blue tetrazolium bromide [3-(4,5-dimethyl-2-thiazolyl)-2,5-diphenyl-2*H*-tetrazolium bromide] (MTT) assay (Datki et al., 2003). SH-SY5Y cells were seeded into 384-well plates at 3,000 cells per well and treated with novel compounds at a concentration of 1 μM, 3 h prior to the addition of $A\beta_{1-42}$ (5 μM). After 24 h of incubation, 5 μl of the MTT reagent (5 mg/ml) was added to each well. 40 μl of DMSO was used to dissolve formazan crystals. Absorbance values were measured at 690 and 570 nm using a BMG Omega Fluorostar microplate reader.

4.2.5 Docking Simulations

Molecular docking simulation was conducted using AutoDock 4.2 (Goodsell et al., 1996). The crystal structures of the studied targets, PDBID: 1EVE (Kryger et al., 1999) and 4BDS (Nachon et al., 2013) for AChE and BuChE, were retrieved from the RCSB protein data bank website. The reason for the selection of these codes was their high resolution, 2.50 and 2.10 Å for 1EVE and 4BDS, respectively. The 3D structures of the potent compounds (**3f** and **3t**) were prepared by Chem3D software. The analysis of docking results was performed by the Discovery Studio software. To validate our docking protocol, re-dock simulations were performed. The results showed that the RMSD values were 0.96 and 0.66 for AChE and BuChE targets, respectively, which confirmed the accuracy of the docking protocol.

DATA AVAILABILITY STATEMENT

The original contributions presented in the study are included in the article/**Supplementary Material**; further inquiries can be directed to the corresponding authors.

AUTHOR CONTRIBUTIONS

This work was part of the Ph.D. thesis of EB, who synthesized and characterized all the compounds and wrote the first draft of the manuscript. LJ-B participated in compound characterization, data analysis, and writing the manuscript. HN performed ChEs inhibition activity. TK and EÖ performed all the analyses regarding the anti-amyloid activity of the compounds. HF and MA assessed the neuroprotective activities of the compounds. EH and LF handled docking simulations. TA participated in the cell toxicity and neuroprotection assays. AF and MS provided lab facilities and participated in data analysis and revision of the manuscript. BM participated in the synthesis of the target compounds and data analysis and gave conceptual advice and edited the manuscript. MK designed and organized the work and handled all processes of the work.

FUNDING

This work was supported by a grant from the Research Council of Tehran University of Medical Sciences and financially by a grant from the National Institute for Medical Research Development (NIMAD), Iran (grant number 977114).

SUPPLEMENTARY MATERIAL

The Supplementary Material for this article can be found online at: https://www.frontiersin.org/articles/10.3389/fchem.2022.895483/full#supplementary-material

REFERENCES

Abdpour, S., Jalili-Baleh, L., Nadri, H., Forootanfar, H., Bukhari, S. N. A., Ramazani, A., et al. (2021). Chromone Derivatives Bearing Pyridinium Moiety as Multi-Target-Directed Ligands against Alzheimer's Disease. *Bioorg. Chem.* 110, 104750. doi:10.1016/j.bioorg.2021.104750

Abdshahzadeh, H., Golshani, M., Nadri, H., Saberi Kia, I., Abdolahi, Z., Forootanfar, H., et al. (2019). 3-Aryl Coumarin Derivatives Bearing Aminoalkoxy Moiety as Multi-Target-Directed Ligands against Alzheimer's Disease. *Chem. Biodivers* 16, e1800436. doi:10.1002/cbdv.201800436

Abu-Aisheh, M. N., Al-Aboudi, A., Mustafa, M. S., El-Abadelah, M. M., Ali, S. Y., Ul-Haq, Z., et al. (2019). Coumarin Derivatives as Acetyl-And Butyrylcholinestrase Inhibitors: An *In Vitro*, Molecular Docking, and Molecular Dynamics Simulations Study. *Heliyon* 5, e01552. doi:10.1016/j.heliyon.2019.e01552

Alcaro, S., Bolognesi, M. L., García-Sosa, A. T., and Rapposelli, S. (2019). Multi-target-directed Ligands (MTDL) as Challenging Research Tools in Drug Discovery: From Design to Pharmacological Evaluation. *Front. Chem.* 7, 71. doi:10.3389/fchem.2019.00071

Altaf, A. A., Shahzad, A., Gul, Z., Khan, S. A., Badshah, A., Tahir, M. N., et al. (2015). A Review on the Medicinal Importance of Pyridine Derivatives. *J. Chem.* 2015, 1–5. doi:10.1155/2015/913435

Anand, P., Singh, B., and Singh, N. (2012). A Review on Coumarins as Acetylcholinesterase Inhibitors for Alzheimer's Disease. *Bioorg. Med. Chem.* 20, 1175–1180. doi:10.1016/j.bmc.2011.12.042

Bagheri, S. M., Khoobi, M., Nadri, H., Moradi, A., Emami, S., Jalili-Baleh, L., et al. (2015). Synthesis and Anticholinergic Activity of 4-hydroxycoumarin Derivatives Containing Substituted Benzyl-1, 2, 3-triazole Moiety. *Chem. Biol. Drug Des.* 86, 1215–1220. doi:10.1111/cbdd.12588

Bilgin, H. M., Atmaca, M., Deniz Obay, B., Özekinci, S., Taşdemir, E., and Ketani, A. (2011). Protective Effects of Coumarin and Coumarin Derivatives against Carbon Tetrachloride-Induced Acute Hepatotoxicity in Rats. *Exp. Toxicol. Pathol.* 63, 325–330. doi:10.1016/j.etp.2010.02.006

Bolognesi, M. L., Bartolini, M., Tarozzi, A., Morroni, F., Lizzi, F., Milelli, A., et al. (2011). Multitargeted Drugs Discovery: Balancing Anti-amyloid and Anticholinesterase Capacity in a Single Chemical Entity. *Bioorg. Med. Chem. Lett.* 21, 2655–2658. doi:10.1016/j.bmcl.2010.12.093

Canning, C., Sun, S., Ji, X., Gupta, S., and Zhou, K. (2013). Antibacterial and Cytotoxic Activity of Isoprenylated Coumarin Mammea A/AA Isolated from Mammea Africana. *J. Ethnopharmacol.* 147, 259–262. doi:10.1016/j.jep.2013.02.026

Cavalli, A., Bolognesi, M. L., Minarini, A., Rosini, M., Tumiatti, V., Recanatini, M., et al. (2008). Multi-target-directed Ligands to Combat Neurodegenerative Diseases. *J. Med. Chem.* 51, 347–372. doi:10.1021/jm7009364

Chen, W.-W., Zhang, X., and Huang, W.-J. (2016). Role of Physical Exercise in Alzheimer's Disease. *Biomed. Rep.* 4, 403–407. doi:10.3892/br.2016.607

Chen, R., Chan, P.-T., Chu, H., Lin, Y.-C., Chang, P.-C., Chen, C.-Y., et al. (2017). Treatment Effects between Monotherapy of Donepezil versus Combination with Memantine for Alzheimer Disease: a Meta-Analysis. *PLoS One* 12, e0183586. doi:10.1371/journal.pone.0183586

Choubdar, N., Golshani, M., Jalili-Baleh, L., Nadri, H., Küçükkilinç, T. T., Ayazgök, B., et al. (2019). New Classes of Carbazoles as Potential Multi-Functional Anti-alzheimer's Agents. *Bioorg. Chem.* 91, 103164. doi:10.1016/j.bioorg.2019.103164

Datki, Z., Juhász, A., Gálfi, M., Soós, K., Papp, R., Zádori, D., et al. (2003). Method for Measuring Neurotoxicity of Aggregating Polypeptides with the MTT Assay on Differentiated Neuroblastoma Cells. *Brain Res. Bull.* 62, 223–229. doi:10.1016/j.brainresbull.2003.09.011

Davidsson, P., Blennow, K., Andreasen, N., Eriksson, B., Minthon, L., and Hesse, C. (2001). Differential Increase in Cerebrospinal Fluid-Acetylcholinesterase after Treatment with Acetylcholinesterase Inhibitors in Patients with Alzheimer's Disease. *Neurosci. Lett.* 300, 157–160. doi:10.1016/S0304-3940(01)01586-5

Du, H., Liu, X., Xie, J., and Ma, F. (2019). Novel Deoxyvasicinone–Donepezil Hybrids as Potential Multitarget Drug Candidates for Alzheimer's Disease. *ACS Chem. Neurosci.* 10, 2397–2407. doi:10.1021/acschemneuro.8b00699

Ellman, G. L., Courtney, K. D., Andres, V., Jr, and Featherstone, R. M. (1961). A New and Rapid Colorimetric Determination of Acetylcholinesterase Activity. *Biochem. Pharmacol.* 7, 88–95. doi:10.1016/0006-2952(61)90145-9

González, J. F., Alcántara, A. R., Doadrio, A. L., and Sánchez-Montero, J. M. (2019). Developments with Multi-Target Drugs for Alzheimer's Disease: an Overview of the Current Discovery Approaches. *Expert Opin. drug Discov.* 14, 879–891. doi:10.1080/17460441.2019.1623201

Goodsell, D. S., Morris, G. M., and Olson, A. J. (1996). Automated Docking of Flexible Ligands: Applications of AutoDock. *J. Mol. Recognit.* 9, 1–5. doi:10.1002/(sici)1099-1352(199601)9:1<1::aid-jmr241>3.0.co;2-6

Hirbod, K., Jalili-Baleh, L., Nadri, H., Ebrahimi, S. E. S., Moradi, A., Pakseresht, B., et al. (2017). Coumarin Derivatives Bearing Benzoheterocycle Moiety: Synthesis, Cholinesterase Inhibitory, and Docking Simulation Study. *Iran. J. Basic Med. Sci.* 20, 631–638. doi:10.22038/IJBMS.2017.8830

Hopkins, A. L. (2008). Network Pharmacology: the Next Paradigm in Drug Discovery. *Nat. Chem. Biol.* 4, 682–690. doi:10.1038/nchembio.118

Inestrosa, N. C., Sagal, J. P., and Colombres, M. (2005). Acetylcholinesterase Interaction with Alzheimer Amyloid β. *Alzheimer's Dis.* 38, 299–317. doi:10.1007/0-387-23226-5_15

Jeremic, D., Jiménez-Díaz, L., and Navarro-López, J. D. (2021). Past, Present and Future of Therapeutic Strategies against Amyloid-β Peptides in Alzheimer's Disease: a Systematic Review. *Ageing Res. Rev.* 72, 101496. doi:10.1016/j.arr.2021.101496

Kapková, P., Alptüzün, V., Frey, P., Erciyas, E., and Holzgrabe, U. (2006). Search for Dual Function Inhibitors for Alzheimer's Disease: Synthesis and Biological Activity of Acetylcholinesterase Inhibitors of Pyridinium-type and Their Aβ Fibril Formation Inhibition Capacity. *Bioorg. Med. Chem.* 14, 472–478. doi:10.1016/j.bmc.2005.08.034

Koyiparambath, V. P., Prayaga Rajappan, K., Rangarajan, T. M., Al-Sehemi, A. G., Pannipara, M., Bhaskar, V., et al. (2021). Deciphering the Detailed Structure–Activity Relationship of Coumarins as Monoamine Oxidase Enzyme Inhibitors—An Updated Review. *Chem. Biol. Drug Des.* 98, 655–673. doi:10.1111/cbdd.13919

Kryger, G., Silman, I., and Sussman, J. L. (1999). Structure of Acetylcholinesterase Complexed with E2020 (Aricept®): Implications for the Design of New Anti-alzheimer Drugs. *Structure* 7, 297–307. doi:10.1016/s0969-2126(99)80040-9

Levine, H., iii (1993). Thioflavine T Interaction with Synthetic Alzheimer's Disease β-amyloid Peptides: Detection of Amyloid Aggregation in Solution. *Protein Sci.* 2, 404–410. doi:10.1002/pro.5560020312

Li, G., Hong, G., Li, X., Zhang, Y., Xu, Z., Mao, L., et al. (2018). Synthesis and Activity towards Alzheimer's Disease *In Vitro*: Tacrine, Phenolic Acid and Ligustrazine Hybrids. *Eur. J. Med. Chem.* 148, 238–254. doi:10.1016/j.ejmech.2018.01.028

Li, K., Jiang, Y., Li, G., Liu, T., and Yang, Z. (2020). Novel Multitarget Directed Tacrine Hybrids as Anti-alzheimer's Compounds Improved Synaptic Plasticity and Cognitive Impairment in APP/PS1 Transgenic Mice. *ACS Chem. Neurosci.* 11, 4316–4328. doi:10.1021/acschemneuro.0c00574

Liu, G., Jiao, Y., Lin, Y., Hao, H., Dou, Y., Yang, J., et al. (2020). Discovery and Biological Evaluation of New Selective Acetylcholinesterase Inhibitors with Anti-aβ Aggregation Activity through Molecular Docking-Based Virtual Screening. *Chem. Pharm. Bull.* 68, 161–166. doi:10.1248/cpb.c19-00927

Marucci, G., Buccioni, M., Ben, D. D., Lambertucci, C., Volpini, R., and Amenta, F. (2021). Efficacy of Acetylcholinesterase Inhibitors in Alzheimer's Disease. *Neuropharmacology* 190, 108352. doi:10.1016/j.neuropharm.2020.108352

Mollazadeh, M., Mohammadi-Khanaposhtani, M., Zonouzi, A., Nadri, H., Najafi, Z., Larijani, B., et al. (2019). New Benzyl Pyridinium Derivatives Bearing 2, 4-dioxochroman Moiety as Potent Agents for Treatment of Alzheimer's Disease: Design, Synthesis, Biological Evaluation, and Docking Study. *Bioorg. Chem.* 87, 506–515. doi:10.1016/j.bioorg.2019.03.012

Murakami, K., Yamaguchi, T., Izuo, N., Kume, T., Hara, H., and Irie, K. (2020). Synthetic and Biophysical Studies on the Toxic Conformer in Amyloid β with the E22Δ Mutation in Alzheimer Pathology. *ACS Chem. Neurosci.* 11, 3017–3024. doi:10.1021/acschemneuro.0c00331

Nachon, F., Carletti, E., Ronco, C., Trovaslet, M., Nicolet, Y., Jean, L., et al. (2013). Crystal Structures of Human Cholinesterases in Complex with Huprine W and Tacrine: Elements of Specificity for Anti-alzheimer's Drugs Targeting Acetyl-And Butyryl-Cholinesterase. *Biochem. J.* 453, 393–399. doi:10.1042/BJ20130013

Nasr, T., Bondock, S., and Youns, M. (2014). Anticancer Activity of New Coumarin Substituted Hydrazide–Hydrazone Derivatives. *Eur. J. Med. Chem.* 76, 539–548. doi:10.1016/j.ejmech.2014.02.026

Patel, D. V., Patel, N. R., Kanhed, A. M., Teli, D. M., Patel, K. B., Gandhi, P. M., et al. (2020). Further Studies on Triazinoindoles as Potential Novel Multitarget-Directed Anti-alzheimer's Agents. *ACS Chem. Neurosci.* 11, 3557–3574. doi:10.1021/acschemneuro.0c00448

Pérez-Cruz, K., Moncada-Basualto, M., Morales-Valenzuela, J., Barriga-González, G., Navarrete-Encina, P., Núñez-Vergara, L., et al. (2018). Synthesis and Antioxidant Study of New Polyphenolic Hybrid-Coumarins. *Arabian J. Chem.* 11, 525–537. doi:10.1016/j.arabjc.2017.05.007

Pradhan, K., Das, G., Mondal, P., Khan, J., Barman, S., and Ghosh, S. (2018). Genesis of Neuroprotective Peptoid from Aβ30–34 Inhibits Aβ Aggregation and AChE Activity. *ACS Chem. Neurosci.* 9, 2929–2940. doi:10.1021/acschemneuro.8b00071

Reddy, E. K., Remya, C., Mantosh, K., Sajith, A. M., Omkumar, R. V., Sadasivan, C., et al. (2017). Novel Tacrine Derivatives Exhibiting Improved Acetylcholinesterase Inhibition: Design, Synthesis and Biological Evaluation. *Eur. J. Med. Chem.* 139, 367–377. doi:10.1016/j.ejmech.2017.08.013

Sang, Z., Wang, K., Han, X., Cao, M., Tan, Z., and Liu, W. (2018). Design, Synthesis, and Evaluation of Novel Ferulic Acid Derivatives as Multi-Target-Directed Ligands for the Treatment of Alzheimer's Disease. *ACS Chem. Neurosci.* 10, 1008–1024. doi:10.1021/acschemneuro.8b00530

Selkoe, D. J., and Hardy, J. (2016). The Amyloid Hypothesis of Alzheimer's Disease at 25 Years. *EMBO Mol. Med.* 8, 595–608. doi:10.15252/emmm.201606210

Sharma, P., Tripathi, A., Tripathi, P. N., Singh, S. S., Singh, S. P., and Shrivastava, S. K. (2019). Novel Molecular Hybrids of N-Benzylpiperidine and 1, 3, 4-oxadiazole as Multitargeted Therapeutics to Treat Alzheimer's Disease. *ACS Chem. Neurosci.* 10, 4361–4384. doi:10.1021/acschemneuro.9b00430

Trambauer, J., Fukumori, A., and Steiner, H. (2020). Pathogenic Aβ Generation in Familial Alzheimer's Disease: Novel Mechanistic Insights and Therapeutic Implications. *Curr. Opin. Neurobiol.* 61, 73–81. doi:10.1016/j.conb.2020.01.011

Vafadarnejad, F., Mahdavi, M., Karimpour-Razkenari, E., Edraki, N., Sameem, B., Khanavi, M., et al. (2018). Design and Synthesis of Novel Coumarin-Pyridinium Hybrids: *In Vitro* Cholinesterase Inhibitory Activity. *Bioorg. Chem.* 77, 311–319. doi:10.1016/j.bioorg.2018.01.013

Vyas, N. A., Singh, S. B., Kumbhar, A. S., Ranade, D. S., Walke, G. R., Kulkarni, P. P., et al. (2018). Acetylcholinesterase and Aβ Aggregation Inhibition by Heterometallic Ruthenium (II)–platinum (II) Polypyridyl Complexes. *Inorg. Chem.* 57, 7524–7535. doi:10.1021/acs.inorgchem.8b00091

Wang, Z., Wang, Y., Li, W., Mao, F., Sun, Y., Huang, L., et al. (2014). Design, Synthesis, and Evaluation of Multitarget-Directed Selenium-Containing Clioquinol Derivatives for the Treatment of Alzheimer's Disease. *ACS Chem. Neurosci.* 5, 952–962. doi:10.1021/cn500119g

Witaicenis, A., Seito, L. N., Da Silveira Chagas, A., de Almeida, L. D., Luchini, A. C., Rodrigues-Orsi, P., et al. (2014). Antioxidant and Intestinal Anti-inflammatory Effects of Plant-Derived Coumarin Derivatives. *Phytomedicine* 21, 240–246. doi:10.1016/j.phymed.2013.09.001

Xuan, Z., Gu, X., Yan, S., Xie, Y., Zhou, Y., Zhang, H., et al. (2021). Dimeric Tacrine (10)-Hupyridone Effectively Combats Alzheimer's Disease as A Multi-Target-Directed Ligand. *ACS Chem. Neurosci.* 12, 2462–2477. doi:10.1021/acschemneuro.1c00182

Yang, Z., Song, Q., Cao, Z., Yu, G., Liu, Z., Tan, Z., et al. (2020). Design, Synthesis and Evaluation of Flurbiprofen-Clioquinol Hybrids as Multitarget-Directed Ligands against Alzheimer's Disease. *Bioorg. Med. Chem.* 28, 115374. doi:10.1016/j.bmc.2020.115374

Zhang, C., Du, Q.-Y., Chen, L.-D., Wu, W.-H., Liao, S.-Y., Yu, L.-H., et al. (2016). Design, Synthesis and Evaluation of Novel Tacrine-Multialkoxybenzene Hybrids as Multi-Targeted Compounds against Alzheimer's Disease. *Eur. J. Med. Chem.* 116, 200–209. doi:10.1016/j.ejmech.2016.03.077

Zou, C., Montagna, E., Shi, Y., Peters, F., Blazquez-Llorca, L., Shi, S., et al. (2015). Intraneuronal APP and Extracellular Aβ Independently Cause Dendritic Spine Pathology in Transgenic Mouse Models of Alzheimer's Disease. *Acta Neuropathol.* 129, 909–920. doi:10.1007/s00401-015-1421-4

Conflict of Interest: The authors declare that the research was conducted in the absence of any commercial or financial relationships that could be construed as a potential conflict of interest.

The handling editor MS declared a shared affiliation with the authors EH, SM, MS, MK at the time of review.

Publisher's Note: All claims expressed in this article are solely those of the authors and do not necessarily represent those of their affiliated organizations, or those of the publisher, the editors, and the reviewers. Any product that may be evaluated in this article, or claim that may be made by its manufacturer, is not guaranteed or endorsed by the publisher.